Title
3D Bioprinting: New Directions in Articular Cartilage Tissue Engineering.

Journal
ACS biomaterials science & engineering, 3(11)

ISSN
2373-9878

Authors
O'Connell, Grace
Garcia, Jeanette
Amir, Jamali

Publication Date
2017-11-01

DOI
10.1021/acsbiomaterials.6b00587

Peer reviewed

3D Bioprinting: New directions in articular cartilage tissue engineering

Journal:	*ACS Biomaterials Science & Engineering*
Manuscript ID	ab-2016-005873.R1
Manuscript Type:	Review
Date Submitted by the Author:	19-Dec-2016
Complete List of Authors:	O'Connell, Grace; University of California, Berkeley, Mechanical Engineering Garcia, Jeannette; IBM Almaden Research Center, Jamali, Amir; UC Davis Medical Center, Department of Orthopaedic Surgery

3D Bioprinting: New directions in articular cartilage tissue engineering

Grace O'Connell[1], Jeanette Garcia[2], Jamali Amir[3]

[1]Department of Mechanical Engineering
University of California, Berkeley
5122 Etcheverry Hall
Berkeley, CA 94720

[2]IBM Research - Almaden
650 Harry Road K17/D2
San Jose, CA 95120

[3]Joint Preservation Institute
2825 J St. #440
Sacramento, CA 95816

Submitted to: Invited Review to ACS Biomaterials Science & Engineering

Corresponding Author:
Grace D. O'Connell, Ph.D.
University of California, Berkeley
Department of Mechanical Engineering
5122 Etcheverry Hall, #1740
Berkeley, CA 94720
ph: 510-642-3739
fx: 510-643-5539
Email: g.oconnell@berkeley.edu

Abstract

Bioprinting is a growing field with significant potential for developing engineered tissues with compositional and mechanical properties that recapitulates healthy native tissue. Much of the current research in tissue and organ bioprinting has focused on complex tissues that require vascularization. Cartilage tissue engineering has been successful in developing *de novo* tissues using homogenous scaffolds. However, as research moves towards clinical application, engineered cartilage will need to maintain homogeneous nutrient diffusion in larger scaffolds and integrate with surrounding tissues. Bioprinting techniques have provided promising results to address these challenges in cartilage tissue engineering. The purpose of this review was to evaluate 3D extrusion-based bioprinting research for developing engineered cartilage. Specifically, we reviewed the potential impact of 3D bioprinting on nutrient diffusion in larger scaffolds, development of scaffolds with spatial variation in cell distribution or mechanical properties, and cultivation of more complex tissues using multiple materials. Finally, we discuss current limitations and challenges in using 3D bioprinting for cartilage tissue engineering and regeneration.

Keywords: three-dimensional bioprinting; articular cartilage; extrusion printing; tissue engineering; regenerative medicine

Introduction

Damaged or degenerated articular cartilage is the leading cause for disability in Americans, resulting in over $30 billion (2009 dollars) in medical costs each year and lost economic productivity[1]. Cells comprise of less than 1% of the tissue volume[2], and the lack of blood supply limits its ability to self heal, making it more challenging to develop regenerative medicine repair strategies[3]. The current gold standard for treating painful osteoarthritic cartilage is a total joint arthroplasty, where the diseased cartilage and the underlying healthy bone are removed and replaced with metal and plastic components. Over a million total joint arthroplasties are performed each year[4], and younger patients (< 45 years) account for 17% of patients with arthritis-attributed activity limitation[5]. However, due to the limited lifespan of implant materials, younger patients delay receiving their first joint replacement, resulting in multiple physician visits for more conservative treatment options, and increasing the overall costs related to treating painful osteoarthritis total[6]. Moreover, as life expectancy has increased, more patients need revision surgeries to replace worn and damaged implants[7].

More recently, biological repair strategies, including autografts or allografts, have provided potential repair strategies for younger patients[8]. Autografts and allografts have been successful in reducing joint pain, maintaining tissue structure, and improving joint functionality; however, both strategies are limited by tissue availability (*e.g.*, donor site morbidity and donor matching)[9]. Alternatively, developing *de novo* tissues in the laboratory through tissue engineering approaches has led to significant advances in potential repair strategies[10]. However, these approaches have been limited to developing simplified smaller analogs of the native tissue.

Additive manufacturing through three-dimensional (3D) printing has gained increasing popularity in many engineering fields, due to the relative ease in acquiring the necessary

equipment and rapid prototyping capabilities[11]. Additive manufacturing techniques have been used for many years to develop acellular scaffolds with macropores for cartilage tissue engineering (Figure 2)[12]. Early studies have used extrusion-based 3D printing without cells to create large scaffolds and full organs, which were seeded with cells after printing. Cell infiltration into these scaffolds is limited to the interstitial spaces and may be limited to the periphery of the scaffold without further modifications to the scaffold material or use of bioreactor[13]. Recently there has been new research in using additive manufacturing techniques for developing engineered tissues and organs with cells encapsulated within the printing material[12a, 14]. Bioprinting is the combination of using additive manufacturing through 3D printing with biocompatible materials and cells. Moreover, using additive manufacturing eliminates the need for developing a solid material throughout the scaffold. Newer approaches aim to encapsulate cells within the biomaterial during the printing process, which provides its own set of advantages and limitations.

To date, bioprinting has been more widely applied to cardiovascular, bone, and skin engineering[15]. However, the advantages in developing larger complex tissue structures through bioprinting are worth investigating for addressing the challenges currently faced by the cartilage tissue-engineering field. The purpose of this review was to evaluate 3D extrusion-based bioprinting research for developing engineered cartilage. Specifically, we reviewed the potential impact of 3D bioprinting on nutrient diffusion in larger scaffolds, development of scaffolds with spatial variation in cell distribution or mechanical properties, and cultivation of more complex tissues using multiple materials. Finally, we discuss current limitations and challenges in using 3D bioprinting for cartilage tissue engineering and regeneration.

Mechanics of Native and Engineered Tissues

The primary function of articular cartilage is to withstand and absorb large complex loads placed on the joint during daily activities. In cell-based tissue engineering approaches, cells are either self-assembled or seeded within a scaffold to cultivate engineered tissues with biochemical and mechanical properties towards healthy native tissues. Scaffold-less approaches rely on a high cell density to develop extracellular matrix over time[16], resulting in a construct with tensile mechanical properties that are comparable to native values and biochemical composition within the range of native cartilage (Table 1)[17]. However, the final construct thickness of self-assembled engineered cartilage is approximately 1.5 mm, which is thinner than many defect sites [17a, 18].

Scaffold based approaches for articular cartilage often relies on soft hydrogels to provide the initial mechanical strength, a base structure for three-dimensional (3D) tissue deposition, to maintain cell morphology, and to encapsulate both the cells and *de novo* tissue[19]. Furthermore, the scaffold can be fabricated to control matrix deposition by altering the scaffold's stiffness or chemical composition[20]. Manufacturing of hydrogel-based scaffolds often includes thermoset casting or ultraviolet light curing. The successes of these approaches has lead to clinical trails of cell-based tissue engineering approaches, with promising early stage results for eliminating pain and reducing the need for total joint replacement. While hydrogel-based scaffolds maintains the round chondrocyte morphology, this approach over simplifies the complex structure of healthy native cartilage, where collagen fiber architecture, mechanical properties, cell mechanics, and biochemical composition varies significantly through the depth of the tissue (Figure 1; Table 1)[3, 21]. This complex architecture has important implications on stress distribution, sliding mechanics, and load transfer to the underlying bone[22].

The superficial zone is important for the low friction coefficient between articulating cartilage surfaces[23] (Table 1 – friction coefficient) and is the first region to experience tissue remodeling or damage from osteoarthritis[24] or excessive wear[25]. Superficial zone collagen fibers are aligned parallel to the direction of sliding and are important for transferring loads during daily activities[26]. Interestingly, the superficial zone thickness is similar across animal species (i.e., from rat to human), suggesting that the superficial zone is critical for cartilage function. Moreover, the mechanical properties of the superficial zone (Table 1 – Surface) differ from the mechanical properties of the deep zone, due to differences in collagen fiber orientation. Therefore, the lack of a superficial zone in engineered cartilage will likely have significant impact on the friction coefficient of engineered cartilage[18a] and the long-term success of engineered cartilage *in vivo*.

As tissue-engineering approaches advance towards clinical applications, there is a growing need for developing subject-specific scaffolds that recapitulates the native mechanical strength, collagen architecture, surface contour, geometry, and morphology of the patient's native joint. It is not clear whether all aspects of cartilage tissue development should be recapitulated in biological repair strategies[27]. However, recent research has suggests that the mechanical strength (Table 1) and collagen architecture are important for stress distribution during physiological loading, such as compression and sliding[21a]. Moreover, implant size, geometry, and morphology of casted scaffolds are limited by the mold itself (e.g., glass slides or 3D printed molds). As the construct size increases, nutrient diffusion becomes a greater issue resulting in non-uniform matrix deposition and mechanical properties, and cell death closer to the center of the construct[28]. Current solutions for improving nutrient diffusion focus on modifying casted scaffolds, resulting in a lot of wasted engineered tissue, and more importantly,

a loss of cells during the fabrication process. Moving towards clinical repair strategies with human chondrocytes or mesenchymal stem cells will be a significant challenge due to the slower proliferation rate of human cells. Therefore, cartilage-engineering strategies will need to be highly efficient with cell usage.

Towards subject-specific geometry and topography

Cartilage tissue engineering has progressed towards developing patient-specific scaffolds. Differences between the thickness of implanted engineered cartilage and the surrounding native tissue will cause stress raisers and alter the stress distribution in the surrounding cartilage, which may lead to degenerative changes[29]. Scaffolds developed from biocompatible materials can be fabricated to match the defect site thickness and geometry.

Cultivation of clinically relevant tissues has been proposed by converting medical images into steriolithography (STL) files, which can be modified in computer aided design (CAD) software[8a, 30]. For example, the underlying boney contour can be acquired through high-resolution magnetic resonance (MR) imaging or micro-computed tomography (μCT) imaging[31]. The images provide boundary and surface contour information about the bone-cartilage interface, as well as cartilage thickness information (MR images). To create a 3D solid model, images are converted to a solid part (i.e., STL file) by either using commercially available software (e.g., Materialise) or freeware offered through various research groups (e.g., SimVascular). Briefly, a 3D volume is created by selecting the cross sectional area of interest in each image slice. The selected areas are connected through the depth of the imaged tissue through linear or spline interpolation (Figure 3A). Finally, the volume can be converted into a solid part that can be further modified using computer-aided design (CAD) software (Figure 3B). Once a 3D solid is imported into CAD software, complex tissue and organ geometries can be developed for

bioprinting[31d]. There are some limitations in using clinical images due to the assumption that the contour of the underlying bone is equivalent to the surface contour of the healthy cartilage (μCT images) and image resolution (MR images). However, alternative methods using laser point imaging to create a 3D scan of a surface[32], is limited for clinical application because the joint would need to be fully exposed for imaging.

Materials used for cartilage tissue engineering

An ideal material for tissue-engineering purposes is biocompatible and provides structural support for cells. Synthetic and natural hydrogels have been widely used for cartilage tissue engineering. Common hydrogel materials include alginate[33], agarose[34], hyaluronic acid (HA)[35], collagen[36], and poly(ε-caprolactone) (PCL)[13d], poly(ethylene) glycol (PEG), gelatin[37], and their combinations[38]. These hydrogels are highly tunable with regards to mechanical properties[39], thermal setting conditions[40], and nano-porosity[41]. Moreover, biomaterials can be modified to deliver chemical stimuli to promote matrix production[42]. Unfortunately, translating past research in tissue engineering with hydrogels is not necessarily transferable to bioprinting, due to the need for shear-thinning properties[43]. For an in-depth review on modifying hydrogel properties for cartilage tissue engineering purposes, the reviewer is directed to other reviews available in the literature[12a, 35a, 44].

In order to effectively print, hydrogels should exhibit non-Newtonian behavior. Thixotropic gels that exhibit shear-thinning properties as they are extruded through a nozzle are ideal for printing. Since not all gels shear-thin, materials must first be evaluated though rheology to determine their behavior when exposed to stresses associated with printing within narrow thermal ranges. Previous studies have shown that materials that exhibit a linear relationship between viscosity and shear rate improves print quality[45]. Therefore, shear thinning behavior will

be another tunable property to consider when deciding on a material for tissue engineering purposes[46]. Furthermore, gels must exhibit stability to temperature ranges for printing, and in some cases reactions within the gels can occur during the printing process.

Currently, PCL and alginate are the most widely used printable materials for cartilage tissue engineering purposes (e.g., [47]). Alginate seeded with chondrocytes or stem cells act to develop *de novo* tissues, while PCL fibers act as a mechanical support for the scaffold. To improve solidification rates during printing, chemical factors have been added to the material either shortly after extrusion from the nozzle or to the hydrogel mixture, modifying material properties after solidification. For example, work by Costantini and coworkers demonstrated large (15 mm thick) scaffolds can be fabricated using alginate combined with a photocurable polymer[48]. Gel solidification during the printing process was performed by exposing recently extruded material to Ca^{2+} ions at the tip of a coaxial-nozzle (Figure 4A). Work by Cui and coworkers demonstrated that polymerization during printing also acts to improve cell viability compared to polymerization after printing is completed[49]. The bulk compressive modulus of these alginate composites ranged from 50-100 kPa, which is much lower than native cartilage, but has been shown to be preferable over stiffer substrates for encouraging cartilage-like matrix production [20]. Similarly, nanocelulose has been added to alginate to increase its viscosity up to 7-fold and improve bioprintability[43, 50]. These studies demonstrate that new materials or hybrid materials will need to be developed to improve bioprinting capabilities.

Photocurable biomaterials are often used for cartilage tissue engineering approaches[51]; however, the approach for printing these materials differs significantly from hydrogels that are printed with extrusion. The majority of 3D bioprinters use extrusion-based approaches that rely on a thermal-based curing; however, newer printer designs, such as the Carbon3D[52], print with

materials that require a photoinitiator. These printers have the advantage of being faster than extrusion based printers, because the entire layer is cured simultaneously before moving onto the next layer. Due to the significant differences in printing processes between extrusion-based bioprinters and ultraviolet light-based printers, we have focused this review paper on engineered cartilage with thermoset biomaterials.

Improving nutrient diffusion through macro-porosity

There has been significant effort in developing new biomaterials with mechanical properties closer to native tissue properties, or to increase the macro-porosity of the scaffold itself to improve nutrient diffusion[12a]. Developing honeycombed structures allow the use of stronger base materials while improving the overall scaffold porosity, which is important for facilitating *de novo* matrix deposition. Macro-pores, on the order of micrometers, can be included in the scaffold design using 3D printing techniques, which provides an increase in porosity that is 1000-fold greater than the porosity of the material itself (e.g., agarose porosity = 200-400 nm)[15k, 31d, 53].

Previous studies have decreased the nutrient path length by adding macro-channels (millimeter length scale) after casting, and this method has been shown to improve matrix deposition and greatly increase the size of engineered cartilage tissues that can be cultivated *in vitro*[28, 31a, 54]. However, including macro-pores or macro-channels within a scaffold significantly decreases the apparent bulk modulus, which is a significant limitation for repair strategies that aim to implant cell-seeded scaffolds shortly after fabrication[55]. A porous structure will need to withstand large compressive stresses before cells produce functional extracellular matrix, which may likely require stiffer biomaterials. For example, the bulk modulus of 2%/wet weight per

volume (wv) agarose (13.5 kPa) with macro-pores may be comparable to the bulk modulus of solid 2%/wv alginate (7.5 kPa)[56].

Adding macro-channels to a scaffold requires removal of 'excess material'; therefore, these techniques require more cells to be cultivated than necessary for the final construct formation. The need for large cell numbers for 3D tissue development increases the time between procedures and increases the cost of treatment (tissue culture related costs). Nowicki and coworkers used a mixed approach between 3D printing and casting to create osteochondral scaffolds with anisotropic macro-pores[53b]. Their work demonstrated that including macro-pores within a scaffold (~100 μm diameter) improved cell adhesion, matrix production, and functional properties. Furthermore, pore anisotropy has been shown to decrease crack propagation, especially if pores are not aligned with the direction of applied load[57]. Bioprinting with sufficient resolution allows for researchers to create macro-channels during the scaffold manufacturing process, decreasing the amount of cells and material needed, which is important for clinical application, where human cells have a slower expansion rate. However, clinical success of engineered cartilage will depend on the long-term stability of biological implants with or without macro-pores[58].

Connecting soft and hard tissues

Focal defects in the joint may only affect the cartilage tissue (chondral defect) or may include damage to the cartilage layer and underlying bone (osteochondral defects). A major challenge of tissue engineering is integrating engineered tissues within the joint space and with surrounding tissues[59]. Engineered osteochondral tissues include a layer of cartilage tissue with a region of boney tissue, providing additional tissue for integration with the native tissue after implantation[60]. However, mechanical properties and biochemical composition of articular

cartilage changes rapidly from the deep zone to the underlying bone, resulting in a significant challenge in the field (Figure 1)[61]. Building upon the clinical successes observed with autograft and allograft osteochondral units, 3D bioprinting of engineered tissues has the potential to develop complex tissues with location dependent mechanical properties.

Successful bioprinting for bone tissue engineering has been performed using alginate with PCL-embedded fibers[32b] as well as PEG in combination with HA or gelain methacrylate[62]. Printed bi-layered acellular scaffolds have been developed with a transition region consisting of an overlapping region of materials rather than a transition between two materials[59c]. To date, there are few studies that used bioprinting techniques to develop a single scaffold with mechanical properties that transition through the thickness to encourage bone growth on one end and cartilage growth at the opposite end[53b]. Studies that have created bioprinted osteochondral constructs have printed materials in close proximity with a clear demarcation between layers, rather than having a graded transition zone[49, 63], which may be due to current printing limitations. However, Shim and coworkers showed that osteochondral scaffolds, created with a PCL structure and bilayered regions for cartilage and bone growth, improves tissue formation and integration with the surrounding tissue[63c]. For in-depth review on current strategies for developing osteochondral scaffolds for tissue engineering (i.e., including non-bioprinting methods), the reader is directed to other reviews available in the literature[64].

Increasing complexity of engineered cartilage

Chondrocytes in the superficial zone are flat and elongated, and are more aligned with the top surface. Chondrocyte morphology and density changes decreases through the thickness of the articular cartilage, where chondrocytes in the middle and deep zones tend to be rounder than chondrocytes in the superficial zone (Figure 1). Bioprinting provides a platform for designing

scaffolds that aim to recapitulate zonal variability in cell density and cell properties[65]. Recent work by Ren *et al.* and Cui *et al.* developed bioprinted scaffolds with spatial variation in cell density[36b, 66]. These studies showed that increasing cell density increased total matrix deposition; however, the rate of extracellular matrix production was higher for cells seeded at a lower density[66]. Similar to bulk material casting, bioprinted hydrogels can be encapsulated with micro- or nano-particles to allow for spatial control of drug and nutrient delivery and increase matrix production[62b, 67].

Printing resolutions range between 5 μm and 100 μm[48], which suggests that a secondary material with stiffer mechanical properties can be incorporated into the printing process to create collagen fiber-like architecture throughout the scaffold thickness. For example, the concentration of Ca^{2+} used to initiate crosslinking in alginate can be modified during printing to alter scaffold stiffness[48, 68]. This strategy may be valuable for developing thicker scaffolds with variability in mechanical properties through the scaffold thickness, similar to differences observed from the superficial zone to the deep zone[69]. Alternatively, multiple materials can be printed where the secondary material is printed within a support structure that is washed away or solidified through a secondary method separate from the support material (Figure 5)[46].

Improving print resolution will need to be balanced with the need to maintain cell viability during printing. Electrospinning techniques have allowed researchers to develop scaffolds with tunable fiber architecture[70], porosity, and stiffness[13a]. However, electrospinning techniques have demonstrated significant challenges in cell encapsulation during printing and with cell infiltration after printing[13a]. Cell encapsulation within hydrogels has been successful; however, printing fibers with a diameter on the micro- or nano-scale will required improved print resolution from current extrusion-based bioprinters. As the nozzle size decreases, the shear stress

on cells passing through the nozzle will increase and may lead to cell apoptosis or inhibit cell behavior[71].

Bioprinting has the potential for increasing complexity of engineered tissues, which will be important for engineered tissue strategies for complex cartilaginous tissues. For example, the intervertebral disc consists of a gelatinous nucleus pulposus surrounded by the annulus fibrosus, which contains alternating layers of highly aligned collagen fibers. Axial compression is the primary loading condition experienced by the disc[72]; therefore, tissue engineering strategies will require materials with similar properties that have been used for cartilage tissue engineering[73]. However, to date, there has been little work in using bioprinting strategies to develop engineered discs or its subcomponents[15k]. A Pubmed search for 'bioprinting' and 'nucleus pulposus', 'intervertebral disc', or 'annulus fibrosus', resulted in only two original research articles using bioprinting techniques to develop an engineered nucleus pulposus[15k] or to create a patient-specific bone insert for spinal fusion[74]. Current tissue engineering approaches cultivate nucleus pulposus implants separate from the annulus fibrosus implant[75]. Modular fabrication results in an abrupt boundary between tissues, which is not representative of the native tissue, and will likely result in inhomogeneous stress distributions[76]. More research is needed to understand how angled 'fibers' can be printed; however, research in bioprinting has demonstrated a great potential for advancing disc tissue engineering, in addition to other cartilaginous tissues.

Current limitations and challenges

As new biomaterials are developed controlling the nozzle head and output speed requires significant tuning, as the rate, nozzle size, and nozzle distance all contribute to print quality and the ability of each additional layer to fuse to the previous layer. Recent work by He and coworkers demonstrated the ability to ejection-print hydrogel material (sodium alginate) with

fibroblasts[77]. Their findings demonstrated a relationship between nozzle height, nozzle pressure, and flow rate on printing accuracy. Future studies that investigate new materials for biomaterial purposes should provide these important parameters, including nozzle temperature, nozzle diameter, and applied pressure, to improve consistency and repeatability of findings across the field (e.g., [77] and [47b]).

Scaffold printing is primarily performed in air; therefore, total printing time is an important consideration for the success of this technique to develop tissue and organs with clinically relevant dimensions. Previous studies have demonstrated that cell viability during and shortly after printing remains high (average construct viability > 85%)[47a, 48, 62a]. He and coworkers demonstrated that bioprinting techniques are capable of creating 15 mm thick scaffolds, but a significant loss in cell viability was noted with printing and may be exacerbated as scaffold geometry increases towards large clinically relevant dimensions[77]. There is conflicting data on whether the initial decrease in cell viability will result in long-term decreases in cell viability and proliferation[47a, 48]. In contrast, cell proliferation in engineered cartilage developed using casting has been shown to increase over time with culture[34a]. Regardless, there has been promising data showing matrix deposition over time and that chondrogenesis of bone-marrow derived mesenchymal stem cells can be achieved in bioprinted scaffolds[48].

Accuracy and printing resolution difficult to control due to the hydrogel material spreading during printing, before solidification is complete (Figure 4B). A recent study by Adamkiewicz and coworkers demonstrated that printing hydrogels in liquid nitrogen reduces thermal stresses during printing, allowing for fabrication of scaffolds with more precisely defined dimensions (Figure 4B)[78]. Printing directly into liquid nitrogen may allow for complex macroporous structures with soft hydrogel materials, but it would limit the ability to print with

cells. It is possible that dimethyl sulfoxide (DMSO) may act as a cryoprotectant to preserve cell viability during printing[79]. However, much of the work on cryopreservation through vitrification has involved methods closer to droplet-based bioprinting than extrusion printing, where freezing characteristics of a droplet are different from a long continuous line. It remains to be seen whether this technique can be transferred over to extrusion-based bioprinting.

Many of the early studies in tissue bioprinting created custom-built printers[36b] or created modifications to commercially available 3D printers[46, 78]. Low-cost ommercially available printers mostly limited to printing with ABS (acrylonitrile butadiene styrene) or PLA by heating the material to very high temperatures (200 - 240^{o}C) before extrusion[80]. For bioprinting, materials that can be printed at temperatures less than 40^{o}C are ideal to prevent cell death during the printing process[36b, 81]. There has been an increase in companies offering commercially available 3D printers for tissue engineering purposes; however, the cost of these printers can exceed $100,000, increasing the total cost related to developing a clinically-relevant biological repair strategy (e.g., BioAssemblyBot by Advanced Solutions ~$160,000 in 2016 dollars)[82]. Newer 3D printers are being developed to print ultraviolet light-curable materials (e.g., Carbon3D, ~$120,000)[52], which have been widely used for cartilage tissue engineering purposes and increases the types of materials that can be used. As demand for these printers increases the prices for alternative 3D bioprinters has already dropped dramatically and will likely continue to decrease (e.g., BioBot Printer; ~$10,000)[83].

Other limitations of 3D bioprinting are limitations shared with tissue engineering approaches, including the risk of cell death during or shortly after implantation[84], obtaining sufficient cell numbers to create subject-specific implants[85], and the amount of time needed to cultivate functional engineered tissue. Furthermore, subject specific repair strategies will likely

require two clinical procedures, where the first one is used to obtain cells and images for scaffold production and the second procedure is used for implantation. It is likely that these procedures will be separated by a period of months as cells are expanded in monolayer culture and used to develop engineered tissues. Techniques, such as priming cells during expansion culture will likely be necessary to increase cell division and *de novo* matrix production[34b, 86].

Conclusions

Bioprinting is a new emerging field with exciting potential to develop engineered tissues with biomimetic properties of healthy native tissues. As with all new emerging technologies there are limitations and challenges that will need to be addressed to increase widespread use of this technology. The early challenges in cartilage bioprinting include developing printable materials that encourage *de novo* cartilage production, printing resolution, maintaining cell viability of large scaffolds, and maintaining scaffold mechanical integrity during printing. In conclusion, bioprinting has the potential to improve engineered tissue complexity and integration to neighboring tissues, spatial dependent properties for cell distribution, substrate stiffness, and scaffold porosity.

Conflict of Interest

The authors certify that there is no conflict of interest related to the work presented in this manuscript.

Table and Figure Legends

Table 1. Mechanical properties of articular cartilage. Bovine cartilage is often used as an animal analog for healthy human cartilage due to limited tissue availability. Compression mechanical properties for bovine cartilage and human cartilage from references [87] and [69b, 88], respectively. Tensile mechanical properties for bovine cartilage from [87a] and for human cartilage from [69b]. Shear mechanical properties for bovine cartilage from [89] and for human cartilage from [69b]. Friction coefficients are from references [23].

Figure 1. (Left) Schematic of cell morphology and collagen fiber orientation from the superficial zone to the deep zone. (Middle) Hematoxylin & Eosin (H&E) stain for cell distribution, and (Right) alcian blue stain for glycosaminoglycan (GAG) distribution demonstrating a transition zone between cartilage and the underlying bone. Figure reprinted with permission from Elsevier [35a].

Figure 2. Scaffolds printed with various macro-porosity and pore geometry. Scale bars represent 1 mm. For scaffold created with cubic pores, the porosity of the scaffold increased from 50% (a) to 68% (b) and 75% (c). Similar increases in macro-porosity are demonstrated for the triangle based pore structure (50% for (d), 68% for (e), and 75% for (f)). Figure adapted from [12a] with permission from Elsevier.

Figure 3. (A) High-resolution micro-computed tomography (μCT) of a human cadaveric tibia plateau. The cross sectional area is manually selected for each slice, and then sections are digitally connected through linear or spline interpolation (SimVascular freeware). (B) The

reconstructed volume was exported from SimVascular as a steriolithography file (STL), which was imported into SolidWorks as a 3D part. The part can be further modified in SolidWorks to identify different material regions or exported for 3D printing. Figure adapted from [31a] with the authors permission.

Figure 4. (A) Coaxial nozzle design to deliver Ca2+ during printing for alginate crosslinking. (B) (Left) 3D cryoprinting setup, where the printing surface is super-cooled with liquid nitrogen. (Right) Printing hydrogels results in a loss of mechanical integrity during the solidification process (asterisks). Printing in liquid nitrogen improves mechanical integrity of the scaffold, allowing for thicker constructs to be printed with increased accuracy in the final dimensions (right corner). Figures adapted from [78] with the author's permission.

Figure 5. Developing more complex tissue structures by injecting a bioink into a support structure. (A) Confocal images of a filament and spiral printed within an unlabeled support gel (black background). (B) (Left) Degradable support gels can be used to create complex self-supporting structures. A covalently crosslinkable bioink was printed within a support gel and solidified with UV crosslinking. Finally, the support gel was dissolved to leave the 3D tetrahedron (Right). Scale bar represents 500 μm. Figure adapted from [46].

References

1. (a) Buckwalter, J. A.; Martin, J. A., Osteoarthritis. *Advanced drug delivery reviews* **2006,** *58* (2), 150-67; (b) Kotlarz, H.; Gunnarsson, C. L.; Fang, H.; Rizzo, J. A., Insurer and out-of-pocket costs of osteoarthritis in the US: evidence from national survey data. *Arthritis and rheumatism* **2009,** *60* (12), 3546-53; (c) Kotlarz, H.; Gunnarsson, C. L.; Fang, H.; Rizzo, J. A., Osteoarthritis and absenteeism costs: evidence from US National Survey Data. *Journal of occupational and environmental medicine / American College of Occupational and Environmental Medicine* **2010,** *52* (3), 263-8.

2. (a) Jadin, K. D.; Wong, B. L.; Bae, W. C.; Li, K. W.; Williamson, A. K.; Schumacher, B. L.; Price, J. H.; Sah, R. L., Depth-varying density and organization of chondrocytes in immature and mature bovine articular cartilage assessed by 3d imaging and analysis. *The journal of histochemistry and cytochemistry : official journal of the Histochemistry Society* **2005,** *53* (9), 1109-19; (b) Sanchez-Adams, J.; Athanasiou, K. A., Biomechanical Characterization of Single Chondrocytes. In *Stud. Mechaniobiol Tissue Eng Biomater*, Springer-Verlag: 2011.

3. Huey, D. J.; Hu, J. C.; Athanasiou, K. A., Unlike bone, cartilage regeneration remains elusive. *Science* **2012,** *338* (6109), 917-21.

4. Brophy, R. H.; Gray, B. L.; Nunley, R. M.; Barrack, R. L.; Clohisy, J. C., Total knee arthroplasty after previous knee surgery: expected interval and the effect on patient age. *The Journal of bone and joint surgery. American volume* **2014,** *96* (10), 801-5.

5. (a) Derman, P. B.; Fabricant, P. D.; David, G., The Role of Overweight and Obesity in Relation to the More Rapid Growth of Total Knee Arthroplasty Volume Compared with Total Hip Arthroplasty Volume. *The Journal of bone and joint surgery. American volume* **2014,** *96* (11), 922-928; (b) Guenther, D.; Schmidl, S.; Klatte, T. O.; Widhalm, H. K.; Omar, M.; Krettek, C.; Gehrke, T.; Kendoff, D.; Haasper, C., Overweight and obesity in hip and knee arthroplasty: Evaluation of 6078 cases. *World journal of orthopedics* **2015,** *6* (1), 137-44; (c) Meehan, J. P.; Danielsen, B.; Kim, S. H.; Jamali, A. A.; White, R. H., Younger age is associated with a higher risk of early periprosthetic joint infection and aseptic mechanical failure after total knee arthroplasty. *The Journal of bone and joint surgery. American volume* **2014,** *96* (7), 529-35; (d) Hootman, J. M.; Helmick, C. G., Projections of US prevalence of arthritis and associated activity limitations. *Arthritis and rheumatism* **2006,** *54* (1), 226-9.

6. Cohen, J. R.; Bradley, A. T.; Lieberman, J. R., Preoperative Interventions and Charges Before Total Knee Arthroplasty. *The Journal of arthroplasty* **2016**.

7. Martin, J. R.; Beahrs, T. R.; Stuhlman, C. R.; Trousdale, R. T., Complex Primary Total Knee Arthroplasty: Long-Term Outcomes. *The Journal of bone and joint surgery. American volume* **2016,** *98* (17), 1459-70.

8. (a) O'Connell, G. D.; Lima, E. G.; Bian, L.; Chahine, N. O.; Albro, M. B.; Cook, J. L.; Ateshian, G. A.; Hung, C. T., Toward engineering a biological joint replacement. *The journal of knee surgery* **2012,** *25* (3), 187-96; (b) Clair, B. L.; Johnson, A. R.; Howard, T., Cartilage repair: current and emerging options in treatment. *Foot & ankle specialist* **2009,** *2* (4), 179-88.

9. (a) Filardo, G.; Kon, E.; Perdisa, F.; Balboni, F.; Marcacci, M., Autologous osteochondral transplantation for the treatment of knee lesions: results and limitations at two years' follow-up. *International orthopaedics* **2014,** *38* (9), 1905-12; (b) Pallante, A. L.; Bae, W. C.; Chen, A. C.; Gortz, S.; Bugbee, W. D.; Sah, R. L., Chondrocyte viability is higher after prolonged storage at 37 degrees C than at 4 degrees C for osteochondral grafts. *The American journal of sports medicine* **2009,** *37 Suppl 1*, 24S-32S; (c) Gortz, S.; Bugbee, W. D., Fresh

osteochondral allografts: graft processing and clinical applications. *The journal of knee surgery* **2006,** *19* (3), 231-40; (d) Huntley, J. S.; Bush, P. G.; McBirnie, J. M.; Simpson, A. H.; Hall, A. C., Chondrocyte death associated with human femoral osteochondral harvest as performed for mosaicplasty. *The Journal of bone and joint surgery. American volume* **2005,** *87* (2), 351-60.

10. (a) Langer, R.; Vacanti, J. P., Tissue engineering. *Science* **1993,** *260* (5110), 920-6; (b) Laurencin, C. T.; Ambrosio, A. M.; Borden, M. D.; Cooper, J. A., Jr., Tissue engineering: orthopedic applications. *Annual review of biomedical engineering* **1999,** *1*, 19-46.

11. Sachs, E.; Cima, M.; Cornie, J.; Brancazio, D.; Bredt, J.; Curodeau, A.; Esterman, M.; Fan, T.; Harris, C.; Kremmin, K.; Lee, S. J.; Pruitt, B.; Williams, P., 3-Dimensional Printing - Rapid Tooling and Prototypes Directly from Cad Representation. *Transactions of the North American Manufacturing Research Institution of Sme 1991* **1991**, 289-296.

12. (a) Hutmacher, D. W., Scaffolds in tissue engineering bone and cartilage. *Biomaterials* **2000,** *21* (24), 2529-43; (b) Hutmacher, D. W.; Sittinger, M.; Risbud, M. V., Scaffold-based tissue engineering: rationale for computer-aided design and solid free-form fabrication systems. *Trends in biotechnology* **2004,** *22* (7), 354-362; (c) Kock, L. M.; Malda, J.; Dhert, W. J.; Ito, K.; Gawlitta, D., Flow-perfusion interferes with chondrogenic and hypertrophic matrix production by mesenchymal stem cells. *Journal of biomechanics* **2014,** *47* (9), 2122-9.

13. (a) Baker, B. M.; Gee, A. O.; Metter, R. B.; Nathan, A. S.; Marklein, R. A.; Burdick, J. A.; Mauck, R. L., The potential to improve cell infiltration in composite fiber-aligned electrospun scaffolds by the selective removal of sacrificial fibers. *Biomaterials* **2008,** *29* (15), 2348-2358; (b) Blakeney, B. A.; Tambralli, A.; Anderson, J. M.; Andukuri, A.; Lim, D. J.; Dean, D. R.; Jun, H. W., Cell infiltration and growth in a low density, uncompressed three-dimensional electrospun nanofibrous scaffold. *Biomaterials* **2011,** *32* (6), 1583-1590; (c) Nerurkar, N. L.; Sen, S.; Baker, B. M.; Elliott, D. M.; Mauck, R. L., Dynamic culture enhances stem cell infiltration and modulates extracellular matrix production on aligned electrospun nanofibrous scaffolds. *Acta biomaterialia* **2011,** *7* (2), 485-491; (d) Moutos, F. T.; Glass, K. A.; Compton, S. A.; Ross, A. K.; Gersbach, C. A.; Guilak, F.; Estes, B. T., Anatomically shaped tissue-engineered cartilage with tunable and inducible anticytokine delivery for biological joint resurfacing. *Proceedings of the National Academy of Sciences of the United States of America* **2016,** *113* (31), E4513-22.

14. Derby, B., Printing and prototyping of tissues and scaffolds. *Science* **2012,** *338* (6109), 921-6.

15. (a) Pati, F.; Song, T. H.; Rijal, G.; Jang, J.; Kim, S. W.; Cho, D. W., Ornamenting 3D printed scaffolds with cell-laid extracellular matrix for bone tissue regeneration. *Biomaterials* **2015,** *37*, 230-41; (b) Jia, W.; Gungor-Ozkerim, P. S.; Zhang, Y. S.; Yue, K.; Zhu, K.; Liu, W.; Pi, Q.; Byambaa, B.; Dokmeci, M. R.; Shin, S. R.; Khademhosseini, A., Direct 3D bioprinting of perfusable vascular constructs using a blend bioink. *Biomaterials* **2016,** *106*, 58-68; (c) Ng, W. L.; Wang, S.; Yeong, W. Y.; Naing, M. W., Skin Bioprinting: Impending Reality or Fantasy? *Trends in biotechnology* **2016,** *34* (9), 689-99; (d) Ozbolat, I. T., Bioprinting scale-up tissue and organ constructs for transplantation. *Trends in biotechnology* **2015,** *33* (7), 395-400; (e) Kolesky, D. B.; Homan, K. A.; Skylar-Scott, M. A.; Lewis, J. A., Three-dimensional bioprinting of thick vascularized tissues. *Proceedings of the National Academy of Sciences of the United States of America* **2016,** *113* (12), 3179-84; (f) Miller, J. S.; Stevens, K. R.; Yang, M. T.; Baker, B. M.; Nguyen, D. H.; Cohen, D. M.; Toro, E.; Chen, A. A.; Galie, P. A.; Yu, X.; Chaturvedi, R.; Bhatia, S. N.; Chen, C. S., Rapid casting of patterned vascular networks for perfusable engineered three-dimensional tissues. *Nature materials* **2012,** *11* (9), 768-74; (g) Duan, B.;

Hockaday, L. A.; Kang, K. H.; Butcher, J. T., 3D bioprinting of heterogeneous aortic valve conduits with alginate/gelatin hydrogels. *Journal of biomedical materials research. Part A* **2013,** *101* (5), 1255-64; (h) Hockaday, L. A.; Kang, K. H.; Colangelo, N. W.; Cheung, P. Y.; Duan, B.; Malone, E.; Wu, J.; Girardi, L. N.; Bonassar, L. J.; Lipson, H.; Chu, C. C.; Butcher, J. T., Rapid 3D printing of anatomically accurate and mechanically heterogeneous aortic valve hydrogel scaffolds. *Biofabrication* **2012,** *4* (3), 035005; (i) Rimann, M.; Bono, E.; Annaheim, H.; Bleisch, M.; Graf-Hausner, U., Standardized 3D Bioprinting of Soft Tissue Models with Human Primary Cells. *Journal of laboratory automation* **2016,** *21* (4), 496-509; (j) Zhao, S.; Zhang, J.; Zhu, M.; Zhang, Y.; Liu, Z.; Tao, C.; Zhu, Y.; Zhang, C., Three-dimensional printed strontium-containing mesoporous bioactive glass scaffolds for repairing rat critical-sized calvarial defects. *Acta biomaterialia* **2015,** *12*, 270-80; (k) Rosenzweig, D. H.; Carelli, E.; Steffen, T.; Jarzem, P.; Haglund, L., 3D-Printed ABS and PLA Scaffolds for Cartilage and Nucleus Pulposus Tissue Regeneration. *International journal of molecular sciences* **2015,** *16* (7), 15118-35; (l) Kang, H. W.; Lee, S. J.; Ko, I. K.; Kengla, C.; Yoo, J. J.; Atala, A., A 3D bioprinting system to produce human-scale tissue constructs with structural integrity. *Nature biotechnology* **2016,** *34* (3), 312-9.

16. Yu, Y.; Moncal, K. K.; Li, J.; Peng, W.; Rivero, I.; Martin, J. A.; Ozbolat, I. T., Three-dimensional bioprinting using self-assembling scalable scaffold-free "tissue strands" as a new bioink. *Scientific reports* **2016,** *6*, 28714.

17. (a) Huang, B. J.; Hu, J. C.; Athanasiou, K. A., Effects of passage number and post-expansion aggregate culture on tissue engineered, self-assembled neocartilage. *Acta biomaterialia* **2016,** *43*, 150-9; (b) Hu, J. C.; Athanasiou, K. A., A self-assembling process in articular cartilage tissue engineering. *Tissue engineering* **2006,** *12* (4), 969-79.

18. (a) Peng, G.; McNary, S. M.; Athanasiou, K. A.; Reddi, A. H., Surface zone articular chondrocytes modulate the bulk and surface mechanical properties of the tissue-engineered cartilage. *Tissue engineering. Part A* **2014,** *20* (23-24), 3332-41; (b) Huang, B. J.; Hu, J. C.; Athanasiou, K. A., Cell-based tissue engineering strategies used in the clinical repair of articular cartilage. *Biomaterials* **2016,** *98*, 1-22.

19. Cao, Y.; Vacanti, J. P.; Paige, K. T.; Upton, J.; Vacanti, C. A., Transplantation of chondrocytes utilizing a polymer-cell construct to produce tissue-engineered cartilage in the shape of a human ear. *Plastic and reconstructive surgery* **1997,** *100* (2), 297-302; discussion 303-4.

20. Bian, L.; Hou, C.; Tous, E.; Rai, R.; Mauck, R. L.; Burdick, J. A., The influence of hyaluronic acid hydrogel crosslinking density and macromolecular diffusivity on human MSC chondrogenesis and hypertrophy. *Biomaterials* **2013,** *34* (2), 413-21.

21. (a) Buckley, M. R.; Gleghorn, J. P.; Bonassar, L. J.; Cohen, I., Mapping the depth dependence of shear properties in articular cartilage. *Journal of biomechanics* **2008,** *41* (11), 2430-7; (b) Wang, C. C.; Chahine, N. O.; Hung, C. T.; Ateshian, G. A., Optical determination of anisotropic material properties of bovine articular cartilage in compression. *Journal of biomechanics* **2003,** *36* (3), 339-53; (c) Oswald, E. S.; Chao, P. H.; Bulinski, J. C.; Ateshian, G. A.; Hung, C. T., Dependence of zonal chondrocyte water transport properties on osmotic environment. *Cellular and molecular bioengineering* **2008,** *1* (4), 339-348; (d) Korhonen, R. K.; Julkunen, P.; Wilson, W.; Herzog, W., Importance of collagen orientation and depth-dependent fixed charge densities of cartilage on mechanical behavior of chondrocytes. *Journal of biomechanical engineering* **2008,** *130* (2), 021003; (e) Verteramo, A.; Seedhom, B. B., Zonal

and directional variations in tensile properties of bovine articular cartilage with special reference to strain rate variation. *Biorheology* **2004,** *41* (3-4), 203-13.

22. (a) Basser, P. J.; Schneiderman, R.; Bank, R. A.; Wachtel, E.; Maroudas, A., Mechanical properties of the collagen network in human articular cartilage as measured by osmotic stress technique. *Archives of biochemistry and biophysics* **1998,** *351* (2), 207-19; (b) Guterl, C. C.; Gardner, T. R.; Rajan, V.; Ahmad, C. S.; Hung, C. T.; Ateshian, G. A., Two-dimensional strain fields on the cross-section of the human patellofemoral joint under physiological loading. *Journal of biomechanics* **2009,** *42* (9), 1275-81.

23. (a) Basalo, I. M.; Chen, F. H.; Hung, C. T.; Ateshian, G. A., Frictional response of bovine articular cartilage under creep loading following proteoglycan digestion with chondroitinase ABC. *Journal of biomechanical engineering* **2006,** *128* (1), 131-4; (b) Henak, C. R.; Ross, K. A.; Bonnevie, E. D.; Fortier, L. A.; Cohen, I.; Kennedy, J. G.; Bonassar, L. J., Human talar and femoral cartilage have distinct mechanical properties near the articular surface. *Journal of biomechanics* **2016,** *49* (14), 3320-3327.

24. Guilak, F.; Ratcliffe, A.; Lane, N.; Rosenwasser, M. P.; Mow, V. C., Mechanical and biochemical changes in the superficial zone of articular cartilage in canine experimental osteoarthritis. *Journal of orthopaedic research : official publication of the Orthopaedic Research Society* **1994,** *12* (4), 474-84.

25. Oungoulian, S. R.; Durney, K. M.; Jones, B. K.; Ahmad, C. S.; Hung, C. T.; Ateshian, G. A., Wear and damage of articular cartilage with friction against orthopedic implant materials. *Journal of biomechanics* **2015,** *48* (10), 1957-64.

26. Bian, L.; Fong, J. V.; Lima, E. G.; Stoker, A. M.; Ateshian, G. A.; Cook, J. L.; Hung, C. T., Dynamic mechanical loading enhances functional properties of tissue-engineered cartilage using mature canine chondrocytes. *Tissue engineering. Part A* **2010,** *16* (5), 1781-90.

27. Bernhard, J. C.; Vunjak-Novakovic, G., Should we use cells, biomaterials, or tissue engineering for cartilage regeneration? *Stem cell research & therapy* **2016,** *7* (1), 56.

28. Bian, L.; Angione, S. L.; Ng, K. W.; Lima, E. G.; Williams, D. Y.; Mao, D. Q.; Ateshian, G. A.; Hung, C. T., Influence of decreasing nutrient path length on the development of engineered cartilage. *Osteoarthritis Cartilage* **2009,** *17* (5), 677-85.

29. Vahdati, A.; Wagner, D. R., Finite element study of a tissue-engineered cartilage transplant in human tibiofemoral joint. *Computer methods in biomechanics and biomedical engineering* **2012,** *15* (11), 1211-21.

30. Hung, C. T.; Lima, E. G.; Mauck, R. L.; Takai, E.; LeRoux, M. A.; Lu, H. H.; Stark, R. G.; Guo, X. E.; Ateshian, G. A., Anatomically shaped osteochondral constructs for articular cartilage repair. *Journal of biomechanics* **2003,** *36* (12), 1853-64.

31. (a) Ford, A.; Chui, W. F.; Zeng, A.; Nandy, A.; Liebenberg, E.; Carraro, C.; Kazakia, G.; Alliston, T.; O'Connell, G. D., Large Modular Engineered Cartilage Surfaces with Evenly Distributed Properties. *J of Tiss Eng and Regn Med* **2016 - In Review**; (b) Cohen, Z. A.; McCarthy, D. M.; Kwak, S. D.; Legrand, P.; Fogarasi, F.; Ciaccio, E. J.; Ateshian, G. A., Knee cartilage topography, thickness, and contact areas from MRI: in-vitro calibration and in-vivo measurements. *Osteoarthritis Cartilage* **1999,** *7* (1), 95-109; (c) Eckstein, F.; Sittek, H.; Milz, S.; Putz, R.; Reiser, M., The morphology of articular cartilage assessed by magnetic resonance imaging (MRI). Reproducibility and anatomical correlation. *Surgical and radiologic anatomy : SRA* **1994,** *16* (4), 429-38; (d) van Uden, S.; Silva-Correia, J.; Correlo, V. M.; Oliveira, J. M.; Reis, R. L., Custom-tailored tissue engineered polycaprolactone scaffolds for total disc replacement. *Biofabrication* **2015,** *7* (1), 015008.

32. (a) Roach, B. L.; Hung, C. T.; Cook, J. L.; Ateshian, G. A.; Tan, A. R., Fabrication of tissue engineered osteochondral grafts for restoring the articular surface of diarthrodial joints. *Methods* **2015,** *84*, 103-8; (b) Daly, A. C.; Cunniffe, G. M.; Sathy, B. N.; Jeon, O.; Alsberg, E.; Kelly, D. J., 3D Bioprinting of Developmentally Inspired Templates for Whole Bone Organ Engineering. *Advanced healthcare materials* **2016,** *5* (18), 2353-62.

33. Wu, Z.; Su, X.; Xu, Y.; Kong, B.; Sun, W.; Mi, S., Bioprinting three-dimensional cell-laden tissue constructs with controllable degradation. *Scientific reports* **2016,** *6*, 24474.

34. (a) O'Connell, G. D.; Nims, R. J.; Green, J.; Cigan, A. D.; Ateshian, G. A.; Hung, C. T., Time and dose-dependent effects of chondroitinase ABC on growth of engineered cartilage. *European cells & materials* **2014,** *27*, 312-20; (b) O'Connell, G. D.; Tan, A. R.; Palmer, G. D.; Cui, V. H.; Bulinski, J. C.; Ateshian, G. A.; Hung, C. T., Cell migration behavior of human chondrocytes for guiding three-dimensional engineered cartilage growth. *Tissue Eng and Regen Med* **2015 - In Press**.

35. (a) Kim, I. L.; Mauck, R. L.; Burdick, J. A., Hydrogel design for cartilage tissue engineering: a case study with hyaluronic acid. *Biomaterials* **2011,** *32* (34), 8771-82; (b) Ifkovits, J. L.; Sundararaghavan, H. G.; Burdick, J. A., Electrospinning fibrous polymer scaffolds for tissue engineering and cell culture. *Journal of visualized experiments : JoVE* **2009,** (32); (c) Prestwich, G. D., Hyaluronic acid-based clinical biomaterials derived for cell and molecule delivery in regenerative medicine. *Journal of controlled release : official journal of the Controlled Release Society* **2011,** *155* (2), 193-9.

36. (a) Zheng, L.; Sun, J.; Chen, X.; Wang, G.; Jiang, B.; Fan, H.; Zhang, X., In vivo cartilage engineering with collagen hydrogel and allogenous chondrocytes after diffusion chamber implantation in immunocompetent host. *Tissue engineering. Part A* **2009,** *15* (8), 2145-53; (b) Ren, X.; Wang, F.; Chen, C.; Gong, X.; Yin, L.; Yang, L., Engineering zonal cartilage through bioprinting collagen type II hydrogel constructs with biomimetic chondrocyte density gradient. *BMC musculoskeletal disorders* **2016,** *17*, 301.

37. (a) Yue, K.; Trujillo-de Santiago, G.; Alvarez, M. M.; Tamayol, A.; Annabi, N.; Khademhosseini, A., Synthesis, properties, and biomedical applications of gelatin methacryloyl (GelMA) hydrogels. *Biomaterials* **2015,** *73*, 254-71; (b) Schuurman, W.; Levett, P. A.; Pot, M. W.; van Weeren, P. R.; Dhert, W. J.; Hutmacher, D. W.; Melchels, F. P.; Klein, T. J.; Malda, J., Gelatin-methacrylamide hydrogels as potential biomaterials for fabrication of tissue-engineered cartilage constructs. *Macromolecular bioscience* **2013,** *13* (5), 551-61.

38. (a) Park, J. S.; Woo, D. G.; Sun, B. K.; Chung, H. M.; Im, S. J.; Choi, Y. M.; Park, K.; Huh, K. M.; Park, K. H., In vitro and in vivo test of PEG/PCL-based hydrogel scaffold for cell delivery application. *Journal of controlled release : official journal of the Controlled Release Society* **2007,** *124* (1-2), 51-9; (b) Singh, Y. P.; Bhardwaj, N.; Mandal, B. B., Potential of Agarose/Silk Fibroin Blended Hydrogel for in Vitro Cartilage Tissue Engineering. *ACS applied materials & interfaces* **2016,** *8* (33), 21236-49; (c) Muller, M.; Becher, J.; Schnabelrauch, M.; Zenobi-Wong, M., Printing thermoresponsive reverse molds for the creation of patterned two-component hydrogels for 3D cell culture. *Journal of visualized experiments : JoVE* **2013,** (77), e50632.

39. Rehfeldt, F.; Engler, A. J.; Eckhardt, A.; Ahmed, F.; Discher, D. E., Cell responses to the mechanochemical microenvironment--implications for regenerative medicine and drug delivery. *Advanced drug delivery reviews* **2007,** *59* (13), 1329-39.

40. Klouda, L.; Mikos, A. G., Thermoresponsive hydrogels in biomedical applications. *European journal of pharmaceutics and biopharmaceutics : official journal of Arbeitsgemeinschaft fur Pharmazeutische Verfahrenstechnik e.V* **2008,** *68* (1), 34-45.
41. (a) Caldorera-Moore, M.; Peppas, N. A., Micro- and nanotechnologies for intelligent and responsive biomaterial-based medical systems. *Advanced drug delivery reviews* **2009,** *61* (15), 1391-401; (b) Annabi, N.; Tamayol, A.; Uquillas, J. A.; Akbari, M.; Bertassoni, L. E.; Cha, C.; Camci-Unal, G.; Dokmeci, M. R.; Peppas, N. A.; Khademhosseini, A., 25th anniversary article: Rational design and applications of hydrogels in regenerative medicine. *Advanced materials* **2014,** *26* (1), 85-123.
42. (a) Sood, N.; Bhardwaj, A.; Mehta, S.; Mehta, A., Stimuli-responsive hydrogels in drug delivery and tissue engineering. *Drug delivery* **2016,** *23* (3), 758-80; (b) Ponnurangam, S.; O'Connell, G. D.; Hung, C. T.; Somasundaran, P., Biocompatibility of polysebacic anhydride microparticles with chondrocytes in engineered cartilage. *Colloids and surfaces. B, Biointerfaces* **2015,** *136*, 207-13.
43. Muller, M.; Ozturk, E.; Arlov, O.; Gatenholm, P.; Zenobi-Wong, M., Alginate Sulfate-Nanocellulose Bioinks for Cartilage Bioprinting Applications. *Annals of biomedical engineering* **2016**.
44. Duarte Campos, D. F.; Drescher, W.; Rath, B.; Tingart, M.; Fischer, H., Supporting Biomaterials for Articular Cartilage Repair. *Cartilage* **2012,** *3* (3), 205-21.
45. Muller, M.; Becher, J.; Schnabelrauch, M.; Zenobi-Wong, M., Nanostructured Pluronic hydrogels as bioinks for 3D bioprinting. *Biofabrication* **2015,** *7* (3), 035006.
46. Highley, C. B.; Rodell, C. B.; Burdick, J. A., Direct 3D Printing of Shear-Thinning Hydrogels into Self-Healing Hydrogels. *Advanced materials* **2015,** *27* (34), 5075-9.
47. (a) Izadifar, Z.; Chang, T.; Kulyk, W.; Chen, X.; Eames, B. F., Analyzing Biological Performance of 3D-Printed, Cell-Impregnated Hybrid Constructs for Cartilage Tissue Engineering. *Tissue engineering. Part C, Methods* **2016,** *22* (3), 173-88; (b) Kundu, J.; Shim, J. H.; Jang, J.; Kim, S. W.; Cho, D. W., An additive manufacturing-based PCL-alginate-chondrocyte bioprinted scaffold for cartilage tissue engineering. *Journal of tissue engineering and regenerative medicine* **2015,** *9* (11), 1286-97.
48. Costantini, M.; Idaszek, J.; Szoke, K.; Jaroszewicz, J.; Dentini, M.; Barbetta, A.; Brinchmann, J. E.; Swieszkowski, W., 3D bioprinting of BM-MSCs-loaded ECM biomimetic hydrogels for in vitro neocartilage formation. *Biofabrication* **2016,** *8* (3), 035002.
49. Cui, X.; Breitenkamp, K.; Finn, M. G.; Lotz, M.; D'Lima, D. D., Direct human cartilage repair using three-dimensional bioprinting technology. *Tissue engineering. Part A* **2012,** *18* (11-12), 1304-12.
50. Markstedt, K.; Mantas, A.; Tournier, I.; Martinez Avila, H.; Hagg, D.; Gatenholm, P., 3D Bioprinting Human Chondrocytes with Nanocellulose-Alginate Bioink for Cartilage Tissue Engineering Applications. *Biomacromolecules* **2015,** *16* (5), 1489-96.
51. (a) Kumar, D.; Gerges, I.; Tamplenizza, M.; Lenardi, C.; Forsyth, N. R.; Liu, Y., Three-dimensional hypoxic culture of human mesenchymal stem cells encapsulated in a photocurable, biodegradable polymer hydrogel: a potential injectable cellular product for nucleus pulposus regeneration. *Acta biomaterialia* **2014,** *10* (8), 3463-74; (b) Metters, A.; Hubbell, J., Network formation and degradation behavior of hydrogels formed by Michael-type addition reactions. *Biomacromolecules* **2005,** *6* (1), 290-301.
52. Carbon3D Carbon3D. http://carbon3d.com/ (accessed 09/16).

53. (a) Pluen, A.; Netti, P. A.; Jain, R. K.; Berk, D. A., Diffusion of macromolecules in agarose gels: comparison of linear and globular configurations. *Biophys J* **1999,** *77* (1), 542-52; (b) Nowicki, M. A.; Castro, N. J.; Plesniak, M. W.; Zhang, L. G., 3D printing of novel osteochondral scaffolds with graded microstructure. *Nanotechnology* **2016,** *27* (41), 414001.
54. (a) Cigan, A. D.; Durney, K. M.; Nims, R. J.; Vunjak-Novakovic, G.; Hung, C. T.; Ateshian, G. A., Nutrient Channels Aid the Growth of Articular Surface-Sized Engineered Cartilage Constructs. *Tissue engineering. Part A* **2016**; (b) Nover, A. B.; Jones, B. K.; Yu, W. T.; Donovan, D. S.; Podolnick, J. D.; Cook, J. L.; Ateshian, G. A.; Hung, C. T., A puzzle assembly strategy for fabrication of large engineered cartilage tissue constructs. *Journal of biomechanics* **2016,** *49* (5), 668-77; (c) Nachemson, A., The Influence of Spinal Movements on the Lumbar Intradiscal Pressure and on the Tensil Stresses in the Annulus Fibrosus. *Acta Orthop Scand* **1963,** *33*, 183-207.
55. DeBerardino, T. M., NeoCart Update: Review of Technique and Early Clinical Results. *Sports medicine and arthroscopy review* **2015,** *23* (3), e23-4.
56. Cloyd, J. M.; Malhotra, N. R.; Weng, L.; Chen, W.; Mauck, R. L.; Elliott, D. M., Material properties in unconfined compression of human nucleus pulposus, injectable hyaluronic acid-based hydrogels and tissue engineering scaffolds. *Eur Spine J* **2007,** *16* (11), 1892-8.
57. Tang, C. A.; Wong, R. H. C.; Chau, K. T.; Lin, P., Modeling of compression-induced splitting failure in heterogeneous brittle porous solids. *Eng Fracture Mech* **2005,** *72*, 597-615.
58. Di Bella, C.; Fosang, A.; Donati, D. M.; Wallace, G. G.; Choong, P. F., 3D Bioprinting of Cartilage for Orthopedic Surgeons: Reading between the Lines. *Frontiers in surgery* **2015,** *2*, 39.
59. (a) Weng, Y.; Cao, Y.; Silva, C. A.; Vacanti, M. P.; Vacanti, C. A., Tissue-engineered composites of bone and cartilage for mandible condylar reconstruction. *Journal of oral and maxillofacial surgery : official journal of the American Association of Oral and Maxillofacial Surgeons* **2001,** *59* (2), 185-90; (b) Yuan, X. L.; Meng, H. Y.; Wang, Y. C.; Peng, J.; Guo, Q. Y.; Wang, A. Y.; Lu, S. B., Bone-cartilage interface crosstalk in osteoarthritis: potential pathways and future therapeutic strategies. *Osteoarthritis Cartilage* **2014,** *22* (8), 1077-89; (c) Taboas, J. M.; Maddox, R. D.; Krebsbach, P. H.; Hollister, S. J., Indirect solid free form fabrication of local and global porous, biomimetic and composite 3D polymer-ceramic scaffolds. *Biomaterials* **2003,** *24* (1), 181-194.
60. Pritzker, K. P.; Gross, A. E.; Langer, F.; Luk, S. C.; Houpt, J. B., Articular cartilage transplantation. *Human pathology* **1977,** *8* (6), 635-51.
61. (a) Yang, P. J.; Temenoff, J. S., Engineering orthopedic tissue interfaces. *Tissue engineering. Part B, Reviews* **2009,** *15* (2), 127-41; (b) Lima, E. G.; Mauck, R. L.; Han, S. H.; Park, S.; Ng, K. W.; Ateshian, G. A.; Hung, C. T., Functional tissue engineering of chondral and osteochondral constructs. *Biorheology* **2004,** *41* (3-4), 577-90.
62. (a) Gao, G.; Schilling, A. F.; Hubbell, K.; Yonezawa, T.; Truong, D.; Hong, Y.; Dai, G.; Cui, X., Improved properties of bone and cartilage tissue from 3D inkjet-bioprinted human mesenchymal stem cells by simultaneous deposition and photocrosslinking in PEG-GelMA. *Biotechnology letters* **2015,** *37* (11), 2349-55; (b) Gao, G.; Schilling, A. F.; Yonezawa, T.; Wang, J.; Dai, G.; Cui, X., Bioactive nanoparticles stimulate bone tissue formation in bioprinted three-dimensional scaffold and human mesenchymal stem cells. *Biotechnology journal* **2014,** *9* (10), 1304-11.
63. (a) Park, J. Y.; Choi, J. C.; Shim, J. H.; Lee, J. S.; Park, H.; Kim, S. W.; Doh, J.; Cho, D. W., A comparative study on collagen type I and hyaluronic acid dependent cell behavior for osteochondral tissue bioprinting. *Biofabrication* **2014,** *6* (3), 035004; (b) Levato, R.; Visser, J.;

Planell, J. A.; Engel, E.; Malda, J.; Mateos-Timoneda, M. A., Biofabrication of tissue constructs by 3D bioprinting of cell-laden microcarriers. *Biofabrication* **2014,** *6* (3), 035020; (c) Shim, J. H.; Jang, K. M.; Hahn, S. K.; Park, J. Y.; Jung, H.; Oh, K.; Park, K. M.; Yeom, J.; Park, S. H.; Kim, S. W.; Wang, J. H.; Kim, K.; Cho, D. W., Three-dimensional bioprinting of multilayered constructs containing human mesenchymal stromal cells for osteochondral tissue regeneration in the rabbit knee joint. *Biofabrication* **2016,** *8* (1), 014102.

64. (a) Nooeaid, P.; Salih, V.; Beier, J. P.; Boccaccini, A. R., Osteochondral tissue engineering: scaffolds, stem cells and applications. *Journal of cellular and molecular medicine* **2012,** *16* (10), 2247-70; (b) Benders, K. E.; van Weeren, P. R.; Badylak, S. F.; Saris, D. B.; Dhert, W. J.; Malda, J., Extracellular matrix scaffolds for cartilage and bone regeneration. *Trends in biotechnology* **2013,** *31* (3), 169-76; (c) Castro, N. J.; Hacking, S. A.; Zhang, L. G., Recent progress in interfacial tissue engineering approaches for osteochondral defects. *Annals of biomedical engineering* **2012,** *40* (8), 1628-40; (d) Nukavarapu, S. P.; Dorcemus, D. L., Osteochondral tissue engineering: current strategies and challenges. *Biotechnology advances* **2013,** *31* (5), 706-21.

65. Murphy, S. V.; Atala, A., 3D bioprinting of tissues and organs. *Nature biotechnology* **2014,** *32* (8), 773-85.

66. Cui, X.; Breitenkamp, K.; Lotz, M.; D'Lima, D., Synergistic action of fibroblast growth factor-2 and transforming growth factor-beta1 enhances bioprinted human neocartilage formation. *Biotechnology and bioengineering* **2012,** *109* (9), 2357-68.

67. Thakur, A.; Jaiswal, M. K.; Peak, C. W.; Carrow, J. K.; Gentry, J.; Dolatshahi-Pirouz, A.; Gaharwar, A. K., Injectable shear-thinning nanoengineered hydrogels for stem cell delivery. *Nanoscale* **2016,** *8* (24), 12362-72.

68. Wan, L. Q.; Jiang, J.; Arnold, D. E.; Guo, X. E.; Lu, H. H.; Mow, V. C., Calcium Concentration Effects on the Mechanical and Biochemical Properties of Chondrocyte-Alginate Constructs. *Cellular and molecular bioengineering* **2008,** *1* (1), 93-102.

69. (a) Schinagl, R. M.; Gurskis, D.; Chen, A. C.; Sah, R. L., Depth-dependent confined compression modulus of full-thickness bovine articular cartilage. *J Orthopaed Res* **1997,** *15* (4), 499-506; (b) Krishnan, R.; Park, S.; Eckstein, F.; Ateshian, G. A., Inhomogeneous cartilage properties enhance superficial interstitial fluid support and frictional properties, but do not provide a homogeneous state of stress. *J Biomech Eng-T Asme* **2003,** *125* (5), 569-577.

70. Matthews, J. A.; Wnek, G. E.; Simpson, D. G.; Bowlin, G. L., Electrospinning of collagen nanofibers. *Biomacromolecules* **2002,** *3* (2), 232-8.

71. (a) Klein, S.; Kuhn, J.; Avrahami, R.; Tarre, S.; Beliavski, M.; Green, M.; Zussman, E., Encapsulation of bacterial cells in electrospun microtubes. *Biomacromolecules* **2009,** *10* (7), 1751-6; (b) Salalha, W.; Kuhn, J.; Dror, Y.; Zussman, E., Encapsulation of bacteria and viruses in electrospun nanofibres. *Nanotechnology* **2006,** *17* (18), 4675-81.

72. (a) O'Connell, G. D.; Malhotra, N. R.; Vresilovic, E. J.; Elliott, D. M., The Effect of Discectomy and the Dependence on Degeneration of Human Intervertebral Disc Strain in Axial Compression. *Spine (Phila Pa 1976)* **2011**; (b) O'Connell, G. D.; Vresilovic, E. J.; Elliott, D. M., Human intervertebral disc internal strain in compression: the effect of disc region, loading position, and degeneration. *Journal of orthopaedic research : official publication of the Orthopaedic Research Society* **2011,** *29* (4), 547-55; (c) O'Connell, G. D.; S., S.; Elliott, D. M., Quantification of The Effect of Degeneration on Annulus Fibrosus Biaxial Mechanics Using a Fiber-induced Anisotropic Hyperelastic Model. *BMMB* **2011**; (d) Beczi, S. E.; Nandy, A.;

O'Connell, G. D., Effect of hydration on healthy intervertebral disc mechanical stiffness. *Journal of biomechanical engineering* **2015** *137* (10).
73. O'Connell, G. D.; Leach, J. K.; Klineberg, E. O., Tissue Engineering a Biological Repair Strategy for Lumbar Disc Herniation. *BioResearch open access* **2015,** *4* (1), 431-45.
74. Serra, T.; Capelli, C.; Toumpaniari, R.; Orriss, I. R.; Leong, J. J.; Dalgarno, K.; Kalaskar, D. M., Design and fabrication of 3D-printed anatomically shaped lumbar cage for intervertebral disc (IVD) degeneration treatment. *Biofabrication* **2016,** *8* (3), 035001.
75. (a) Martin, J. T.; Milby, A. H.; Chiaro, J. A.; Kim, D. H.; Hebela, N. M.; Smith, L. J.; Elliott, D. M.; Mauck, R. L., Translation of an engineered nanofibrous disc-like angle-ply structure for intervertebral disc replacement in a small animal model. *Acta biomaterialia* **2014,** *10* (6), 2473-81; (b) Mizuno, H.; Roy, A. K.; Vacanti, C. A.; Kojima, K.; Ueda, M.; Bonassar, L. J., Tissue-engineered composites of anulus fibrosus and nucleus pulposus for intervertebral disc replacement. *Spine (Phila Pa 1976)* **2004,** *29* (12), 1290-7; discussion 1297-8.
76. O'Connell, G. D.; Hung, C. T.; Ateshian, G. A. In *Experimental and Theoretical Evaluation of Failure Properties for Immature Tissue Engineered Cartilage*, ASME Summer Bioengineering Conference, Farmington, PA, Farmington, PA, 2011.
77. He, Y.; Yang, F.; Zhao, H.; Gao, Q.; Xia, B.; Fu, J., Research on the printability of hydrogels in 3D bioprinting. *Scientific reports* **2016,** *6*, 29977.
78. Adamkiewicz, M.; Rubinsky, B., Cryogenic 3D printing for tissue engineering. *Cryobiology* **2015,** *71* (3), 518-21.
79. (a) Demirci, U.; Montesano, G., Cell encapsulating droplet vitrification. *Lab on a chip* **2007,** *7* (11), 1428-33; (b) Dou, R.; Saunders, R. E.; Mohamet, L.; Ward, C. M.; Derby, B., High throughput cryopreservation of cells by rapid freezing of sub-mul drops using inkjet printing--cryoprinting. *Lab on a chip* **2015,** *15* (17), 3503-13; (c) Landa, V.; Tepla, O., Cryopreservation of mouse 8-cell embryos in microdrops. *Folia biologica* **1990,** *36* (3-4), 153-8; (d) Papis, K.; Shimizu, M.; Izaike, Y., Factors affecting the survivability of bovine oocytes vitrified in droplets. *Theriogenology* **2000,** *54* (5), 651-8.
80. Filaments.ca Starter Temperatures & Printing Guide. https://filaments.ca/pages/temperature-guide (accessed 09/19).
81. Bakarich, S. E.; Panhuis, M. I. H.; Beirne, S.; Wallace, G. G.; Spinks, G. M., Extrusion printing of ionic-covalent entanglement hydrogels with high toughness. *J Mater Chem B* **2013,** *1* (38), 4939-4946.
82. Solutions, A. http://www.bioassemblybot.com/ (accessed 09/19).
83. BioBot BioBots 1. https://http://www.biobots.io/biobot-1/ (accessed 09/19).
84. Borazjani, B. H.; Chen, A. C.; Bae, W. C.; Patil, S.; Sah, R. L.; Firestein, G. S.; Bugbee, W. D., Effect of impact on chondrocyte viability during insertion of human osteochondral grafts. *The Journal of bone and joint surgery. American volume* **2006,** *88* (9), 1934-43.
85. Athanasiou, K. A.; Eswaramoorthy, R.; Hadidi, P.; Hu, J. C., Self-organization and the self-assembling process in tissue engineering. *Annual review of biomedical engineering* **2013,** *15*, 115-36.
86. Sampat, S. R.; O'Connell, G. D.; Fong, J. V.; Aguaron, E. A.; Ateshian, G. A.; Hung, C. T., Growth factor priming of synovium derived stem cells for cartilage tissue engineering. *Tissue engineering. Part A* **2011,** *17* (17-18), 2259-65.
87. (a) Chahine, N. O.; Wang, C. C.; Hung, C. T.; Ateshian, G. A., Anisotropic strain-dependent material properties of bovine articular cartilage in the transitional range from tension to compression. *Journal of biomechanics* **2004,** *37* (8), 1251-61; (b) Wang, C. C.; Deng, J. M.;

Ateshian, G. A.; Hung, C. T., An automated approach for direct measurement of two-dimensional strain distributions within articular cartilage under unconfined compression. *Journal of biomechanical engineering* **2002,** *124* (5), 557-67; (c) Ateshian, G. A.; Warden, W. H.; Kim, J. J.; Grelsamer, R. P.; Mow, V. C., Finite deformation biphasic material properties of bovine articular cartilage from confined compression experiments. *Journal of biomechanics* **1997,** *30* (11-12), 1157-64; (d) Chen, S. S.; Falcovitz, Y. H.; Schneiderman, R.; Maroudas, A.; Sah, R. L., Depth-dependent compressive properties of normal aged human femoral head articular cartilage: relationship to fixed charge density. *Osteoarthritis Cartilage* **2001,** *9* (6), 561-9.

88. Chen, X.; Zhou, Y.; Wang, L.; Santare, M. H.; Wan, L. Q.; Lu, X. L., Determining Tension-Compression Nonlinear Mechanical Properties of Articular Cartilage from Indentation Testing. *Annals of biomedical engineering* **2016,** *44* (4), 1148-58.

89. (a) Griffin, D. J.; Vicari, J.; Buckley, M. R.; Silverberg, J. L.; Cohen, I.; Bonassar, L. J., Effects of enzymatic treatments on the depth-dependent viscoelastic shear properties of articular cartilage. *Journal of orthopaedic research : official publication of the Orthopaedic Research Society* **2014,** *32* (12), 1652-7; (b) Silverberg, J. L.; Barrett, A. R.; Das, M.; Petersen, P. B.; Bonassar, L. J.; Cohen, I., Structure-function relations and rigidity percolation in the shear properties of articular cartilage. *Biophys J* **2014,** *107* (7), 1721-30.

	Compression							
	Young's Modulus (MPa)		Poisson's Ratio		Aggregate Modulus, H_{A0} (MPa)		Permeability ($x10^{-15}$ $m^4N^{-1}s^{-1}$)	
Bovine	Surface	0.1 - 0.5 0.2	Surface	0.05 - 0.13 0.04	Surface	0.27 ± 0.10	Surface	4.55 ± 1.18
	Middle	0.5 - 1.0	Middle	0.13 - 0.15	Middle	0.51 ± 0.31	Middle	1.46 ± 0.83
	Deep	1.0 - 2.0 0.4	Deep	0.15 - 0.20 0.06	Deep	0.71 ± 0.09	Deep	0.50 ± 0.39
					Full Thickness	0.47 ± 0.11 0.40 ± 0.14	Full Thickness	7.30 ± 1.72 2.7 ± 1.5
Human	Surface	0.28 ± 0.16			Full Thickness	0.44 ± 0.24	Full Thickness	0.99
	Deep	0.73 ± 0.26						

	Tension				Shear		Friction	
	Young's Modulus (MPa)		*Poisson's Ratio*		*Shear Modulus (|G*|, MPa)*		Friction Coefficient	
Bovine	Surface	0.1	Surface	0.1	Surface	0.8 - 1.5 0.1 - 0.8	Cartilage - Glass	0.0037 ± 0.0013 0.15 - 0.35
	Deep	0.2	Deep	0.2	Deep	2.0 - 4.0 1 - 5		
Human	Surface	8.3 ± 3.7			Full Thickness	2 - 3	Cartilage - Cartilage	0.001 - 0.03
	Deep	4.9 ± 1.9						

Mechanical properties of articular cartilage. Bovine cartilage is often used as an animal analog for healthy human cartilage due to limited tissue availability. Compression mechanical properties for bovine cartilage and human cartilage from references 87 and 69b, 88, respectively. Tensile mechanical properties for bovine cartilage from 87a and for human cartilage from 69b. Shear mechanical properties for bovine cartilage from 89 and for human cartilage from 69b. Friction coefficients are from references 23.

Table 1

254x109mm (150 x 150 DPI)

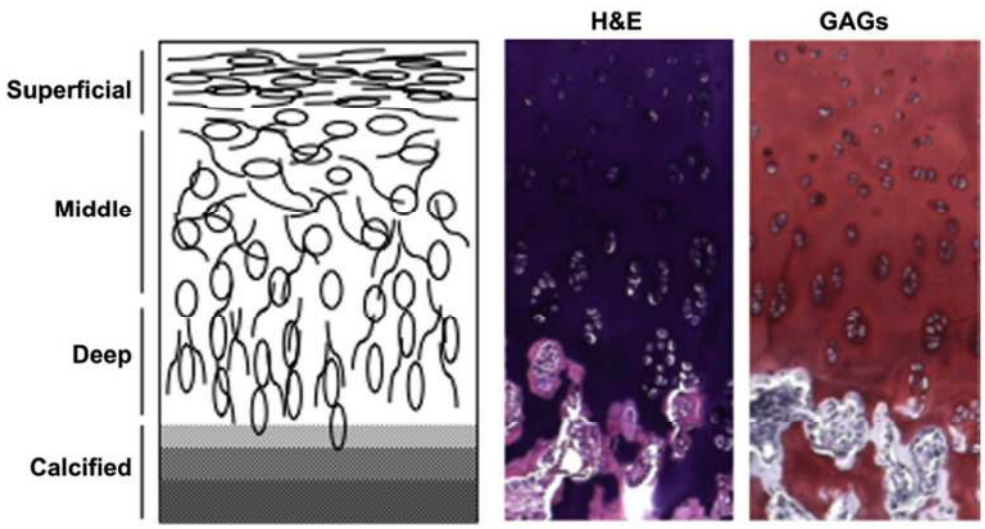

Figure 1. (Left) Schematic of cell morphology and collagen fiber orientation from the superficial zone to the deep zone. (Middle) Hematoxylin & Eosin (H&E) stain for cell distribution, and (Right) alcian blue stain for glycosaminoglycan (GAG) distribution demonstrating a transition zone between cartilage and the underlying bone. Figure reprinted with permission from Elsevier 33a.
Figure 1
197x103mm (300 x 300 DPI)

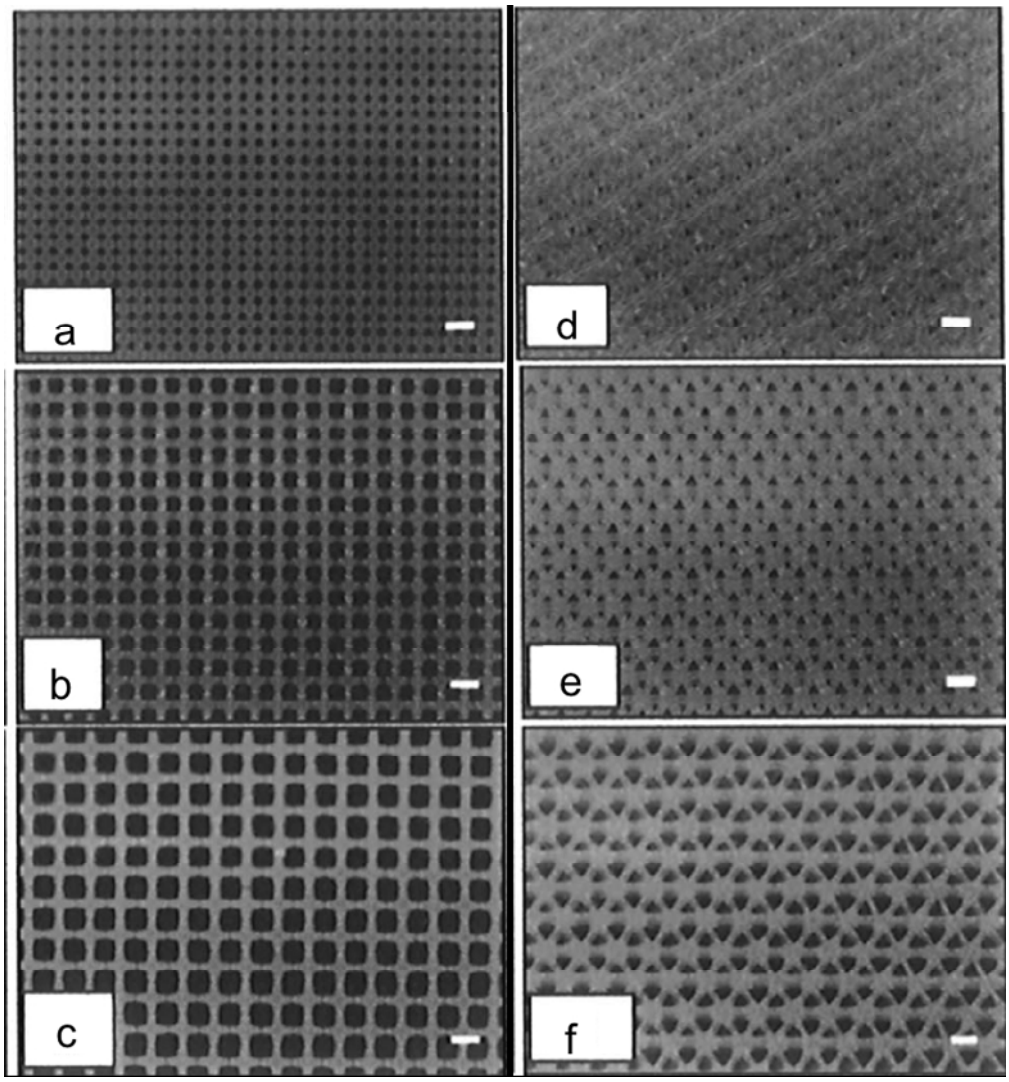

Figure 2. Scaffolds printed with various macro-porosity and pore geometry. Scale bars represent 1 mm. For scaffold created with cubic pores, the porosity of the scaffold increased from 50% (a) to 68% (b) and 75% (c). Similar increases in macro-porosity are demonstrated for the triangle based pore structure (50% for (d), 68% for (e), and 75% for (f)). Figure adapted from 25a with permission from Elsevier.
Figure 2
82x88mm (300 x 300 DPI)

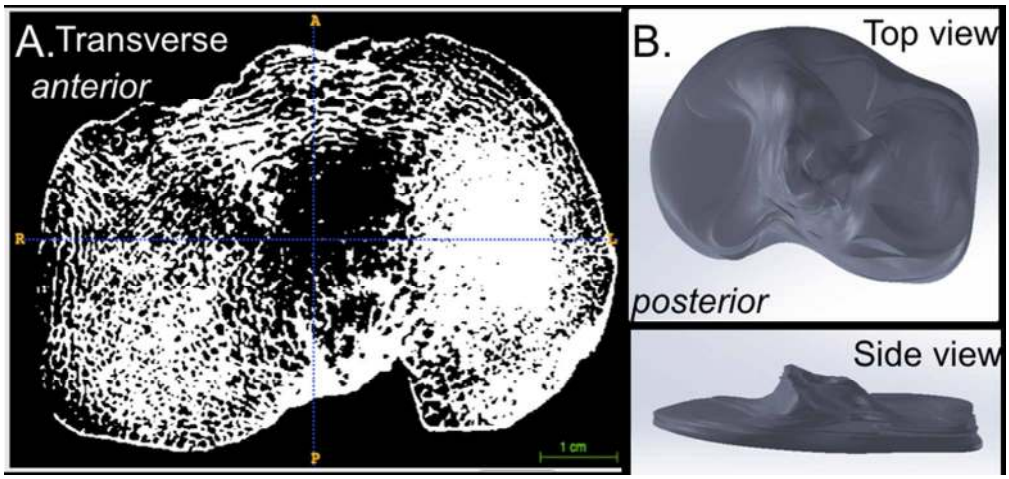

Figure 3. (A) High-resolution micro-computed tomography (μCT) of a human cadaveric tibia plateau. The cross sectional area is manually selected for each slice, and then sections are digitally connected through linear or spline interpolation (SimVascular freeware). (B) The reconstructed volume was exported from SimVascular as a steriolithography file (STL), which was imported into SolidWorks as a 3D part. The part can be further modified in SolidWorks to identify different material regions or exported for 3D printing. Figure adapted from 30a with the authors permission.

Figure 3
82x38mm (300 x 300 DPI)

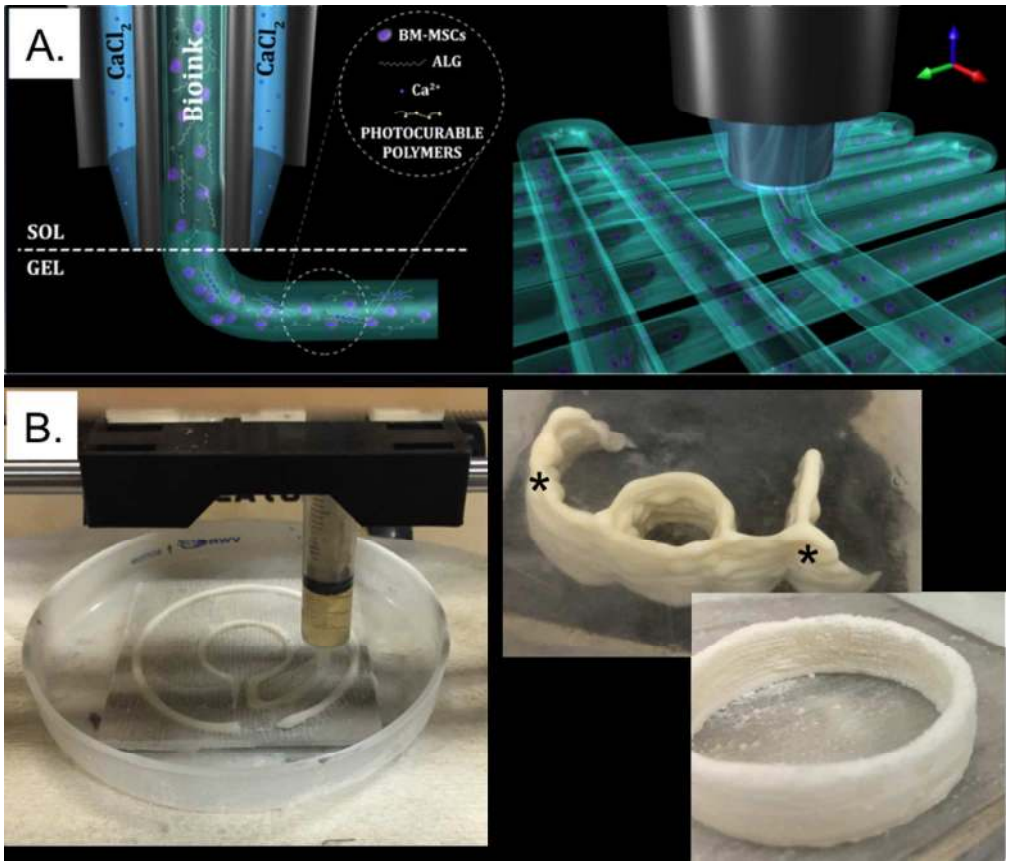

Figure 4. (A) Coaxial nozzle design to deliver Ca2+ during printing for alginate crosslinking. (B) (Left) 3D cryoprinting setup, where the printing surface is super-cooled with liquid nitrogen. (Right) Printing hydrogels results in a loss of mechanical integrity during the solidification process (asterisks). Printing in liquid nitrogen improves mechanical integrity of the scaffold, allowing for thicker constructs to be printed with increased accuracy in the final dimensions (right corner). Figures adapted from 65 with the author's permission.

Figure 4
147x126mm (300 x 300 DPI)

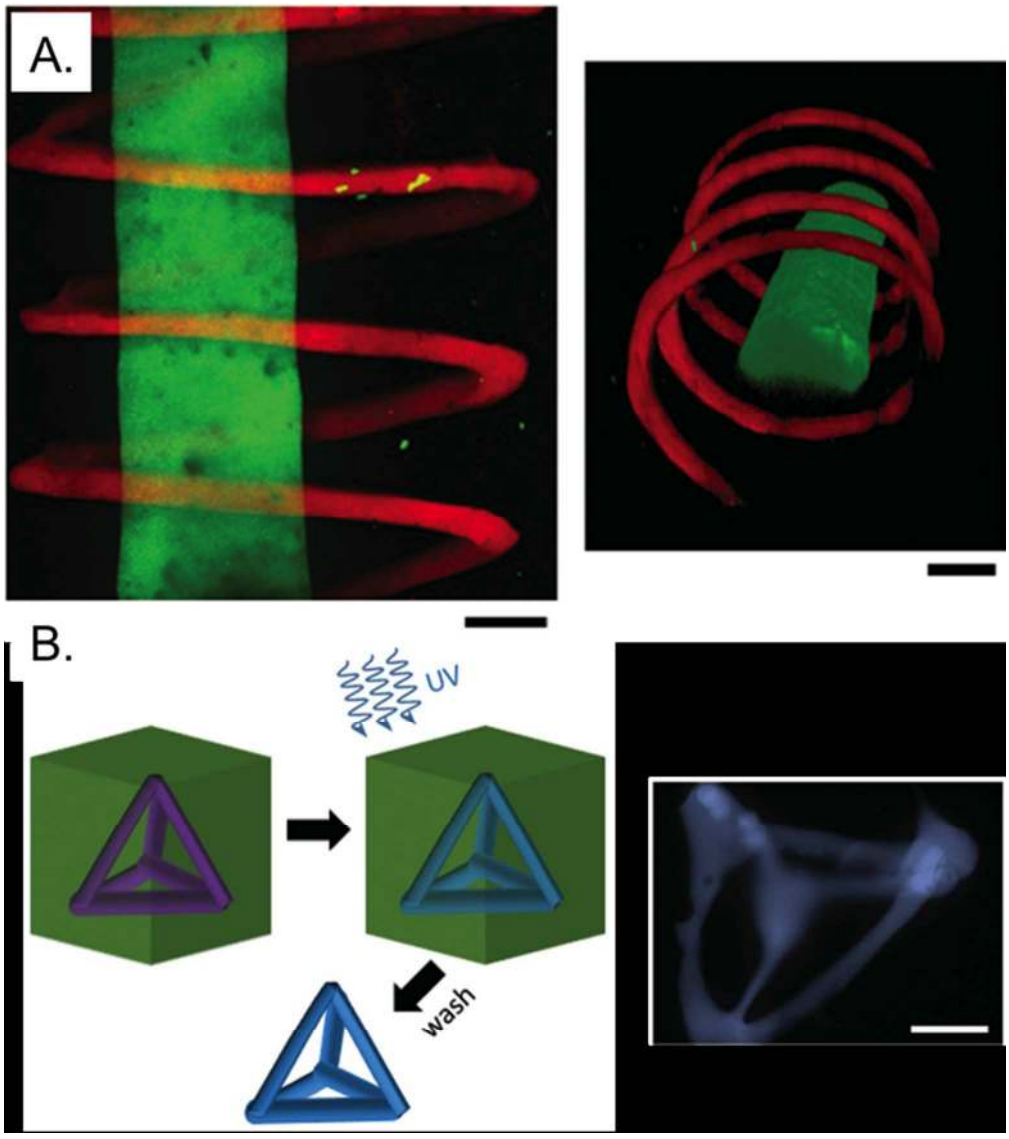

Figure 5. Developing more complex tissue structures by injecting a bioink into a support structure. (A) Confocal images of a filament and spiral printed within an unlabeled support gel (black background). (B) (Left) Degradable support gels can be used to create complex self-supporting structures. A covalently crosslinkable bioink was printed within a support gel and solidified with UV crosslinking. Finally, the support gel was dissolved to leave the 3D tetrahedron (Right). Scale bar represents 500 μm. Figure adapted from 41.

Figure 5
82x93mm (300 x 300 DPI)

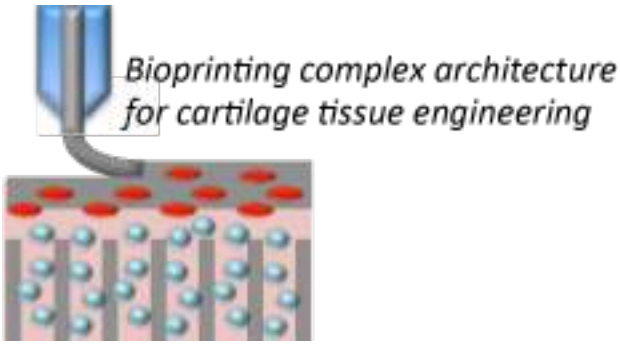
Bioprinting complex architecture
for cartilage tissue engineering

Bioprinting complex architecture for cartilage tissue engineering